

Experimental VLE data of methyl acetate or ethyl acetate + 1-butanol at 0.6 MPa. Predictions with Peng-Robinson EOS and group contribution models

P. Susial*, D. García-Vera, R. Susial and Y.C. Clavijo

Escuela de Ingenierías Industriales y Civiles. Universidad de Las Palmas de Gran Canaria, 35017
Las Palmas de Gran Canaria, Canary Islands, Spain.

Datos experimentales del ELV para acetato de metilo o acetato de etilo + 1-butanol a 0.6 MPa. Predicciones utilizando Peng-Robinson EoS y los modelos de contribución por grupos.

Dades experimentals de l'ELV per l'acetat de metil o acetat d'etil + 1-butanol a 0,6 MPa. Prediccions utilitzant Peng-Robinson EoS i els models d'aportació per grups.

RECEIVED: 5 SEPTEMBER 2017; REVISED: 14 DESEMBER 2017; ACCEPTED: 19 JANUARY 2018

SUMMARY

Vapor-liquid equilibrium data were obtained with a stainless steel ebulliometer at 0.6 MPa for methyl acetate + 1-butanol and ethyl acetate + 1-butanol. The experimental data for the binary systems were tested and verified thermodynamically, showed positive consistency when the point-to-point test of Van Ness was applied. The group contribution models ASOG and three versions of the UNIFAC were applied to calculate the vapor-liquid equilibrium data and after, these values were compared to the experimental data. The approach ϕ - ϕ was applied by using the Peng-Robinson equation of state, the classical attractive term was employed. The quadratic and Wong-Sandler mixing rules were verified and the adjustable parameter of Stryjek-Vera was also applied.

Keywords VLE isobaric data, Methyl Acetate, Ethyl Acetate, 1-Butanol

RESUMEN

Los datos del equilibrio líquido-vapor para el acetato de metilo + 1-butanol y el acetato de etilo + 1-butanol fueron obtenidos a 0.6 MPa utilizando un ebullómetro de acero inoxidable. Los datos experimentales de los sistemas binarios fueron comprobados y verificados termodinámicamente, observándose que presentan consistencia positiva al ser aplicado el test punto a punto de Van Ness. Los modelos de contribución

por grupos ASOG y tres versiones de UNIFAC fueron empleados para calcular los datos del equilibrio líquido-vapor, posteriormente los valores calculados fueron comparados con los datos experimentales. La aproximación ϕ - ϕ fue utilizada aplicando la ecuación de estado de Peng-Robinson, utilizando el término atractivo clásico. Las reglas de mezclado cuadráticas y las de Wong-Sandler fueron verificadas y se empleó el parámetro ajustable de Stryjek-Vera.

Palabras clave: Datos isobáricos del ELV; acetato de metilo; acetato de etilo; 1-butanol.

RESUM

Les dades de l'equilibri líquid-vapor per a l'acetat de metil + 1-butanol i l'acetat d'etil + 1-butanol es van obtenir a 0,6 MPa utilitzant un ebullòscopi d'acer inoxidable. Les dades experimentals dels sistemes binaris es van comprovar i verificar termodinàmicament, i es va observar que presenten consistència positiva a l'aplicació del test de Van Ness punt a punt. Els models d'aportació per grups ASOG i les tres versions de UNIFAC van ser emprats per calcular les dades de l'equilibri líquid-vapor, i posteriorment els valors calculats van ser comparats amb els dades experimentals. L'aproximació ϕ - ϕ es va utilitzar aplicant

* Corresponding author: psusial@dip.ulpgc.es

l'equació d'estat de Peng-Robinson, utilitzant el terme atractiu clàssic. Les regles de barrejat quadràtiques i les de Wong-Sandler van ser verificades i es va utilitzar el paràmetre ajustable de Stryjek-Vera.

Paraules clau: Dades isobàriques de l'ELV; acetat de metil; acetat de etil; 1-butanol.

INTRODUCTION

Esters and alcohols are frequently used in different industrial processes. Methyl acetate is used in organic synthesis and is also an excellent solvent for resin and paints, while ethyl acetate is used in the food, photographic, textile and paper industries. 1-butanol is employed in chlorination processes, as a dehydrating agent, in paints, lacquers and varnishes; in the pharmaceutical industry, for tanning of hides, in the photographic industry and in perfumes. 1-butanol has also been studied as biodiesel due to the energy demand.

Consequently, the study of the behavior of these substances, mixtures and the determination of the vapor-liquid equilibrium (VLE) has a scientific interest and is necessary in many industrial processes. That is why as in previous works^{1,2} we determined VLE data for ester/alcohol binary mixtures at moderate pressure. Data were determined at 0.6 MPa for (1) methyl acetate + (2) 1-butanol (MA1B) and (1) ethyl acetate + (2) 1-butanol (EA1B). These systems were previously studied by different authors³⁻⁶ under several operating conditions.

VLE of MA1B has been studied at 74.66 and 127.99 kPa by Susial and Ortega³, at 101.3 kPa by Belousov et al.³, Esteller et al.³, Ortega and Susial³, and Patlasov et al.⁴; and at 0.3 MPa by Susial et al.⁵. VLE of EA1B has been studied isothermally by Alsmeyer and Marquardt³ and isobarically at 70.5 and 94 kPa by Darwish and Al-Khateib³, at 97.3 kPa by Mainkar and Mene⁶ at 101.3 kPa by Belousov et al.³, Ortega et al.⁴ and Shono et al.⁴; and at 0.3 MPa by Susial et al.⁵. Azeotropes have not been reported in these systems.

In this study experimental data were verified by applying the test of Van Ness⁷ using the FORTRAN program⁸ of Fredenslund et al. The γ - ϕ approach enables to analyze the efficiency of the different group contribution models⁹⁻¹². In addition, by using the ϕ - ϕ approach, experimental data were correlated with the Peng-Robinson¹³ (PR) equation of state (EOS) using quadratic mixing rules or Wong-Sandler¹⁴ (WS) mixing rules. The classical attractive term or the adjustable parameter of Stryjek-Vera¹⁵ (SV) were also used in both cases.

EXPERIMENTAL

Chemicals

Methyl acetate, ethyl acetate and 1-butanol (99%, 99.9% and 99.9% mass purity, respectively) from Panreac Química S.A. were used. The physical properties, normal boiling point (T_{bp}), density (ρ_{ii}) and refractive index (n_D) at 298.15 K have been previously published^{1,2,5}. These products were used as received.

A Kyoto Electronics DA-300 vibrating tube density meter with an uncertainty of $\pm 0.1 \text{ kg}\cdot\text{m}^{-3}$ was employed for density determinations of both pure components and VLE data. In addition, a Zusi 315RS Abbe refractometer with an uncertainty of ± 0.0002 units was used for the refractive index determinations of pure components.

Equipment and procedures

An ebulliometer made of stainless steel (2 mm thickness) was employed (Fig. 1) to obtain experimental VLE data. The apparatus operates with a 400 cm³ capacity. It has been built to work at moderate or high pressures. Flooding does not occur when working with about 800 cm³ of mixing liquid. The liquid mixture is heated in a double-walled inverted vessel (E). Liquid and vapor circulate due to the Cottrell pump effect that takes place when the liquid is heated inside the boiling flask (E). The liquid phase is circulated across the funnel (B) to be collected in the C valve. The condensed vapor in the cooler (F) is circulated to be collected in the D valve.

The general description of the equilibrium ebulliometer and the disposal of the different elements in the installation can be consulted in previous papers^{1,2,5}.

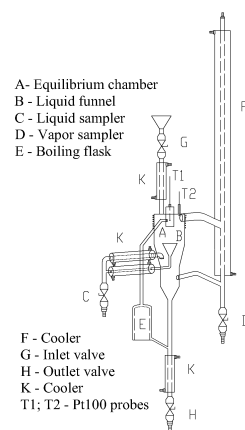


Fig. 1. Schematic diagram of the equilibrium recirculation still used for VLE measurements.

The experiments began with the cleaning of the equipment. For this, about 500 cm³ of ethanol were introduced in the ebulliometer and the electric resistance located at E (see Fig. 1) was switched on; ethanol was boiled and kept under recirculation at atmospheric pressure for 45 min. After this, ethanol was removed and, with the equipment still hot, the system was left under vacuum at 10 kPa (absolute pressure) for 45 min. Next, the ebulliometer was loaded with about 500 cm³ of acetone and the electric resistance located at E (see Fig. 1) was turned on; boiling of acetone was maintained under recirculation for 45 min at atmospheric pressure. Thereafter, acetone was removed and before the equipment cooled, vacuum was applied at 10 kPa (absolute pressure) for 45 min. Finally, the ebulliometer was closed at negative pressure (taking manometric pressure as reference), and dry nitrogen was introduced using a separate line¹ until a pressure of about 150 kPa was reached. Before loading the equipment with the substances to be studied, pressure was reduced to 101 kPa; this enables to introduce the substances without contamination. Next, the equip-

ment was closed and charged with dry nitrogen, ready to operate at moderate pressure^{1,2,5,16}.

The equilibrium still typology is of those in which both phases are recirculated. The ebullimeter operates dynamically by using the vapor lift pump effect. The equipment is made to work in co-currents flow, and thus, the equilibrium condition depends on the contact time between the non-miscible phases: the mass transfer process is a function of residence time. In other words, the equilibrium condition does not only depend on constant temperature and pressure. Consequently, the statistical value of these two properties cannot be taken as the equilibrium criterion; the constant composition of both phases must be also verified.

For this ebullimeter, the input/output flow of each phase was evaluated under different operating conditions and with different binary mixtures¹⁶. With a flow around 25 cm³/min it was possible to obtain a composition in each phase that remained practically constant when the renovation time was greater than 75 min. For this reason, the mixtures studied in this work were kept at boiling conditions for 90 min to ensure the stationary state. Once the steady state was reached the vapor and liquid phase were both sampled. Next, the equilibrium was disturbed by adding one of the substances to the mixture in the ebullimeter.

A digital recorder Dostmann Electronic GmbH p655 and two Pt100 probes with ±0.03 K uncertainty were employed. The calibration of the system was done by Dostmann Electronic GmbH. Proper operation of the probes installed in the equipment was verified by measuring the boiling point of distilled water. Pressure was controlled with a pressure regulating valve (Binks MFG Co.) included in the nitrogen supply line. Pressure was measured with a digital transducer 8311 from Burket Fluid Control Systems, with an operating range from 0.0 to 4.0 MPa (uncertainty ±0.004 MPa).

A calibration curve of composition vs. density had been previously obtained at 298.15 K for the systems of this work⁵. Mole fraction (x_i) vs. density (ρ_i) data were verified by the adequate correlation of the excess volumes. The uncertainty was estimated to be less than 0.003 in mole fraction of vapor phase.

RESULTS AND DISCUSSION

Treatment and Prediction of VLE data

The VLE data T - x_1 - y_1 for MA1B and EA1B at 0.6 MPa are shown in Table 1. The activity coefficients of the liquid phase (γ_i) for each system were determined by using the following equation:

$$\gamma_i = \frac{y_i p}{x_i p_i} \exp \left[\frac{p}{RT} \left(2 \sum_j y_j B_{ij} - \sum_i \sum_j y_i y_j B_{ij} \right) - \frac{p_i^o B_{ii}}{RT} + \frac{(p_i^o - p) v_i^L}{RT} \right] \quad (1)$$

The virial state equation truncated at the second term was employed and the second virial coefficients (B_{ii} , B_{ij}) were obtained by means of the Hayden and O'Connell¹⁷ method (see Table 1). The liquid molar volumes of pure compounds were estimated from the equation of Yen and Woods¹⁸. Table 1 includes the γ_i values calculated

from VLE data and using Eq. 1 as was previously indicated and by using the properties of Table 2. Literature data^{1,20,21} were employed to obtain the Antoine constants (see Table 2). A moderate positive deviation from Raoult's Law can be observed, probably due to a molecular association via hydrogen bonds.

Table 1 Experimental VLE data for binary systems at 0.6 MPa. Calculated values of second virial coefficients and activity coefficients of the liquid phase^a

T	x_1	y_1	B_{11}	B_{22}	B_{12}	γ_1	γ_2
K			L/mol	L/mol	L/mol		
methyl acetate (1) + 1-butanol (2)							
452.24	0.000	0.000	-0.4855	-0.5675			1.00
448.61	0.034	0.108	-0.4958	-0.5855	-0.5426	1.05	1.00
448.17	0.036	0.116	-0.4970	-0.5877	-0.5442	1.07	1.00
447.31	0.044	0.140	-0.4995	-0.5921	-0.5474	1.08	1.00
446.09	0.054	0.175	-0.5031	-0.5985	-0.5520	1.12	1.00
444.77	0.068	0.213	-0.5070	-0.6056	-0.5570	1.11	1.00
444.40	0.072	0.224	-0.5081	-0.6076	-0.5584	1.11	1.00
443.38	0.084	0.251	-0.5111	-0.6132	-0.5624	1.08	1.01
441.51	0.100	0.290	-0.5168	-0.6236	-0.5697	1.08	1.02
439.49	0.120	0.343	-0.5230	-0.6353	-0.5778	1.11	1.02
436.74	0.151	0.416	-0.5317	-0.6517	-0.5891	1.12	1.00
435.16	0.166	0.437	-0.5368	-0.6615	-0.5957	1.10	1.03
433.67	0.186	0.476	-0.5416	-0.6710	-0.6021	1.10	1.02
433.02	0.192	0.486	-0.5438	-0.6752	-0.6049	1.11	1.03
427.78	0.259	0.599	-0.5614	-0.7108	-0.6284	1.11	1.01
425.72	0.288	0.635	-0.5686	-0.7257	-0.6380	1.11	1.01
423.03	0.323	0.678	-0.5782	-0.7459	-0.6509	1.11	1.01
417.51	0.418	0.761	-0.5987	-0.7907	-0.6786	1.07	1.03
417.11	0.425	0.762	-0.6002	-0.7941	-0.6807	1.07	1.05
415.14	0.456	0.784	-0.6078	-0.8114	-0.6911	1.06	1.07
413.56	0.492	0.802	-0.6140	-0.8257	-0.6996	1.04	1.10
413.19	0.501	0.801	-0.6155	-0.8291	-0.7017	1.03	1.14
410.07	0.578	0.837	-0.6281	-0.8588	-0.7191	1.00	1.22
406.15	0.659	0.880	-0.6444	-0.8988	-0.7420	1.00	1.26
404.97	0.690	0.893	-0.6495	-0.9115	-0.7491	0.99	1.29
402.47	0.753	0.914	-0.6604	-0.9394	-0.7645	0.98	1.41
401.16	0.790	0.926	-0.6662	-0.9546	-0.7728	0.98	1.49
400.18	0.812	0.937	-0.6707	-0.9662	-0.7791	0.98	1.47
397.34	0.895	0.963	-0.6837	-1.0013	-0.7978	0.98	1.70
396.45	0.920	0.971	-0.6879	-1.0128	-0.8038	0.98	1.81
396.02	0.931	0.974	-0.6899	-1.0184	-0.8067	0.98	1.91
395.56	0.943	0.977	-0.6921	-1.0244	-0.8099	0.98	2.08
395.01	0.956	0.984	-0.6947	-1.0318	-0.8137	0.99	1.91
394.91	0.961	0.986	-0.6952	-1.0331	-0.8144	0.98	1.89
394.33	0.974	0.990	-0.6979	-1.0409	-0.8184	0.99	2.07
394.10	0.979	0.991	-0.6991	-1.0441	-0.8200	0.99	2.32
393.01	1.000	1.000	-0.7043	-1.0592			1.00

^a Expanded uncertainties U(0.95 level of confidence) are: U(T)=0.03 K, U(p)= 0.004 MPa, U(x_1)=U(y_1)=0.003

VLE data were tested for thermodynamic consistency by using the point-to-point test of Van Ness et al.⁷ Results indicate that the experimental data for MA1B and EA1B binary systems at 0.6 MPa satisfy the Fredenslund et al.⁸ criterion. Results of the Redlich-Kister and Herington test were respectively: D=75.97 > 10% and ABS(D-J)=53.36 > 10 for MA1B; D=59.50 > 10% and ABS(D-J)=46.83 > 10 for EA1B. Therefore both system fails with area test. In addition, bibliographic³⁻⁵ data were employed for data verification of this work, and for this purpose all data were correlated to a polynomial equation presented in a previous paper¹⁶ as follows,

$$y_1 - x_1 = x_1(1 - x_1) \sum_{k=0}^K A_k Z_T^k \quad \text{with} \quad Z_T = \frac{x_1}{x_1 + R_T(1 - x_1)} \quad (2)$$

being A_k and R_T adjustable parameters. The fitting curves and experimental data are shown in Figs. 2 and

3. A significant compressive effect can be observed as a consequence of the applied pressure. Data from this study agrees with that in literature³⁻⁵.

Table 1 Continued^a

T	x_1	y_1	B_{11}	B_{22}	B_{12}	Y_1	Y_2
K			L/mol	L/mol	L/mol		
ethyl acetate (1) + 1-butanol (2)							
452.24	0.000	0.000	-0.6539	-0.5675			1.00
451.47	0.008	0.018	-0.6566	-0.5712	-0.6220	1.13	1.00
451.31	0.013	0.025	-0.6571	-0.5720	-0.6227	0.97	1.00
450.82	0.018	0.044	-0.6588	-0.5744	-0.6247	1.24	1.00
450.66	0.023	0.049	-0.6594	-0.5752	-0.6253	1.08	1.00
450.11	0.034	0.073	-0.6613	-0.5779	-0.6276	1.10	1.00
449.13	0.050	0.108	-0.6648	-0.5828	-0.6317	1.13	1.00
447.81	0.069	0.147	-0.6695	-0.5896	-0.6373	1.14	1.01
446.97	0.089	0.180	-0.6726	-0.5939	-0.6409	1.10	1.01
445.99	0.105	0.214	-0.6761	-0.5991	-0.6452	1.13	1.01
445.12	0.123	0.245	-0.6793	-0.6037	-0.6490	1.12	1.01
444.25	0.139	0.268	-0.6825	-0.6084	-0.6528	1.11	1.02
443.27	0.158	0.298	-0.6861	-0.6138	-0.6572	1.10	1.03
441.18	0.202	0.365	-0.6940	-0.6255	-0.6666	1.10	1.04
437.30	0.284	0.478	-0.7089	-0.6483	-0.6848	1.11	1.05
436.66	0.301	0.506	-0.7114	-0.6522	-0.6878	1.12	1.03
434.05	0.363	0.570	-0.7218	-0.6685	-0.7005	1.10	1.06
431.25	0.433	0.642	-0.7331	-0.6869	-0.7146	1.10	1.07
429.17	0.496	0.691	-0.7417	-0.7010	-0.7253	1.08	1.10
427.48	0.565	0.738	-0.7488	-0.7129	-0.7341	1.05	1.13
426.96	0.584	0.749	-0.7527	-0.7195	-0.7390	1.05	1.16
425.24	0.649	0.790	-0.7584	-0.7292	-0.7462	1.02	1.20
424.6	0.674	0.808	-0.7612	-0.7340	-0.7497	1.02	1.20
423.98	0.701	0.829	-0.7639	-0.7387	-0.7531	1.02	1.18
423.83	0.709	0.827	-0.7645	-0.7398	-0.7539	1.01	1.24
423.49	0.727	0.835	-0.7660	-0.7424	-0.7558	1.00	1.27
423.07	0.750	0.854	-0.7679	-0.7456	-0.7581	1.00	1.24
422.52	0.777	0.863	-0.7703	-0.7499	-0.7612	0.99	1.33
422.05	0.798	0.879	-0.7724	-0.7536	-0.7639	0.99	1.31
421.89	0.806	0.887	-0.7731	-0.7548	-0.7648	0.99	1.28
421.30	0.830	0.899	-0.7757	-0.7595	-0.7681	0.99	1.33
420.02	0.880	0.925	-0.7814	-0.7698	-0.7755	0.99	1.45
418.70	0.938	0.957	-0.7874	-0.7807	-0.7831	0.99	1.68
418.00	0.964	0.976	-0.7906	-0.7866	-0.7873	0.99	1.64
417.82	0.976	0.983	-0.7915	-0.7881	-0.7883	0.99	1.76
417.58	0.982	0.988	-0.7926	-0.7901	-0.7898	1.00	1.67
417.33	0.990	0.994	-0.7937	-0.7923	-0.7912	1.00	1.51
417.02	1.000	1.000	-0.7951	-0.7923			1.00

^a Expanded uncertainties $U(0.95$ level of confidence) are: $U(T)=0.03$ K, $U(p)=0.004$ MPa, $U(x_i)=U(y_i)=0.003$

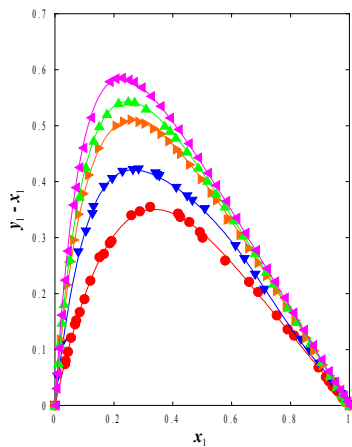


Fig. 2 Plot of experimental (y_1-x_1) vs. x_1 data for MA1B (●) at 0.6 MPa. Literature data at 74.66 (◀) and 127.99 (▶) kPa by Susial and Ortega³, 101.3 (▲) kPa by Ortega and Susial³, and 0.3 (▼) MPa by Susial et al.⁵ with fitting curves.

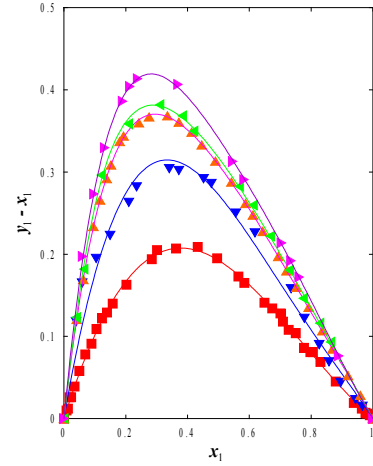


Fig. 3 Experimental points of (y_1-x_1) vs. x_1 for EA1B (■) at 0.6 MPa. Literature data at 70.5 (◀) and 94.0 (▲) kPa by Darwish and Al-Khateib³, 101.3 (▶) kPa by Ortega et al.⁴ and 0.3 (▼) MPa by Susial et al.⁵ with fitting curves.

Next, considering the excess Gibbs function,

$$\frac{G^E}{RT} = x_1 \ln \gamma_1 + x_2 \ln \gamma_2 \quad (3)$$

the activity coefficients were correlated with the following thermodynamic models: the Wilson²² model, the NRTL²³ model and the UNIQUAC²⁴ model.

In the Wilson model²² the excess Gibbs function is represented by the following equation,

$$\frac{G^E}{RT} = -x_1 \ln(x_1 + \Lambda_{12}x_2) - x_2 \ln(x_2 + \Lambda_{21}x_1) \quad \text{with} \quad \Lambda_{ij} = \frac{V_j}{V_i} \exp\left(-\frac{\Delta\lambda_{ij}}{RT}\right) \quad (4)$$

where the Wilson functions Λ_{ij} depends on the adjustable interaction energy parameters $\Delta\lambda_{ij}$ and the molar volumes of pure components, V_i and V_j , which have been calculated with the Yen and Woods¹⁸ equation (see Table 2).

The NRTL model²³ applies the following equation for the excess Gibbs free energy,

$$\frac{G^E}{RT} = x_1 x_2 \left(\frac{G_{21}\tau_{21}}{x_1 + G_{21}x_2} + \frac{G_{12}\tau_{12}}{x_2 + G_{12}x_1} \right) \quad \text{with} \quad G_{ij} = \exp(-\alpha_{ij}\tau_{ij}) \quad \text{and} \quad \tau_{ij} = \frac{\Delta g_{ij}}{RT} \quad (5)$$

where $\alpha_{ij} = \alpha_{ji}$ is a non-random parameter of the mixture which is associated with molecular organization. The adjustable parameters, τ_{ij} , depend on a temperature function with interaction energies Δg_{ij} between an i - j pair of molecules.

In the UNIQUAC model²⁴ the excess Gibbs function is composed of the combinatorial and residual parts as follow,

$$\frac{G^E}{RT} = \frac{G_{Comb}^E}{RT} + \frac{G_{Resid}^E}{RT} \quad (6)$$

$$\frac{G_{Comb}^E}{RT} = x_1 \ln\left(\frac{\Phi_1}{x_1}\right) + x_2 \ln\left(\frac{\Phi_2}{x_2}\right) + \left(\frac{Z}{2}\right) \left[q_1 x_1 \ln\left(\frac{\theta_1}{\Phi_1}\right) + q_2 x_2 \ln\left(\frac{\theta_2}{\Phi_2}\right) \right] \quad (7)$$

Table 2 Properties of literature¹⁹ and from this work.

Tc ¹⁹ K	Pc ¹⁹ MPa	RD ¹⁹ Å	μ ¹⁹ D	Zc ¹⁹	A	B	C	V _i L/mol	r	q
506.80	4.69	2.996	1.679	0.254	6.7347	1529.38	6.59	0.0798	2.8042	2.576
523.25	3.83	3.468	1.781	0.252	7.0337	1869.43	-22.19	0.0985	3.4786	3.116
562.93	4.4127	3.251	1.66	0.259	6.4296	1261.325	106.43	0.0936	3.4543	3.052

$$\log_{10} P_i^o \text{ kPa} = A - \frac{B}{TK - C}$$

Table 3 Correlation parameters of G^E/RT vs. x_p , mean absolute deviations and standard deviations

model	parameters	MAD(γ_i)	MAD(T)/K	SD(γ_1)	SD(γ_2)	SD(G^E/RT)
methyl acetate (1) + 1-butanol (2) at 0.6 MPa						
Wilson ²²	$\Delta\lambda_{12} = -2824.4 \text{ J}\cdot\text{mol}^{-1}$ $\Delta\lambda_{21} = 6962.7 \text{ J}\cdot\text{mol}^{-1}$	0.019	2.04	0.11	0.14	0.015
NRTL ($\alpha = 0.47$) ²³	$\Delta g_{12} = 5996.6 \text{ J}\cdot\text{mol}^{-1}$ $\Delta g_{21} = -2183.6 \text{ J}\cdot\text{mol}^{-1}$	0.018	2.04	0.10	0.12	0.018
UNIQUAC ($Z = 10$) ²⁴	$\Delta u_{12} = 3935.6 \text{ J}\cdot\text{mol}^{-1}$ $\Delta u_{21} = -2104.9 \text{ J}\cdot\text{mol}^{-1}$	0.020	2.07	0.11	0.14	0.016
ethyl acetate (1) + 1-butanol (2) at 0.6 MPa						
Wilson ²²	$\Delta\lambda_{12} = -1693.4 \text{ J}\cdot\text{mol}^{-1}$ $\Delta\lambda_{21} = 4206.9 \text{ J}\cdot\text{mol}^{-1}$	0.013	0.53	0.07	0.09	0.010
NRTL ($\alpha = 0.47$) ²³	$\Delta g_{12} = 4396.8 \text{ J}\cdot\text{mol}^{-1}$ $\Delta g_{21} = -1896.1 \text{ J}\cdot\text{mol}^{-1}$	0.013	0.61	0.07	0.08	0.012
UNIQUAC ($Z = 10$) ²⁴	$\Delta u_{12} = 3185.2 \text{ J}\cdot\text{mol}^{-1}$ $\Delta u_{21} = -1922.2 \text{ J}\cdot\text{mol}^{-1}$	0.014	0.57	0.07	0.09	0.011

$$\text{MAD}(F) = \frac{1}{n-2} \sum_{i=1}^n |F_{\text{exp}} - F_{\text{cal}}|; \quad \text{SD}(F) = \sqrt{\frac{\sum_{i=1}^n (F_{\text{exp}} - F_{\text{cal}})^2}{n-2}}; \quad F = \gamma_i, T, p, \gamma_1, \gamma_2, G^E/RT$$

$$\frac{G_{\text{Resid}}^E}{RT} = -q_1 x_1 \ln(\theta_1 + \theta_2 \tau_{21}) - q_2 x_2 \ln(\theta_2 + \theta_1 \tau_{12}) \quad (8)$$

$$\Phi_i = \frac{x_i r_i}{x_i r_i + x_j r_j}; \quad \theta_i = \frac{x_i q_i}{x_i q_i + x_j q_j} \quad \text{and} \quad \tau_{ij} = \exp\left(-\frac{\Delta u_{ij}}{RT}\right) \quad (9)$$

being Z the coordination number, Φ the molecular fraction of segments and θ the molecular fraction of surfaces. τ_{ij} are the adjustable parameters and Δu_{ij} represents the average interaction energy of molecules. The volume and area of groups of van der Waals are used to calculate r and q , volume and area parameters, of the UNIQUAC model (see Table 2).

The adjustable parameters in each of these models (Table 3) were obtained using the Nelder and Mead method²⁵. Deviation in the sum of the squares of activity coefficient was minimized for both substances during optimization of the parameters. For MA1B the NRTL equation²³ yielded the lowest mean absolute deviations (MAD) as well as standard deviations (SD) between experimental and calculated values for temperature and vapor compositions. However, the Wilson model²² yields the best correlation for EA1B, with the lowest MAD in both temperature and vapor phase mole fraction.

Temperature, pressure, vapor phase composition and the calculated activity coefficients were compared with the theoretical predictions of VLE obtained with the ASOG model⁹, the mod. UNIFAC-Lyngby model¹⁰ proposed by Larsen et al., the original UNIFAC model⁸ with Hansen et al. parameters¹¹ and the mod. UNIFAC-Dortmund model¹² proposed by Gmehling et al.

In the group contribution models the activity coefficient of the liquid phase are calculated with the following equation:

$$\ln \gamma_i = \ln \gamma_i^{\text{Comb}} + \ln \gamma_i^{\text{Resid}} \quad (10)$$

Differences in the models arise from the interpretation given in each one about the combinatorial and residual contributions. In the ASOG⁹ model the combinatorial part is obtained by using the Flory-Huggins equation

$$\ln \gamma_i^{\text{Comb}} = 1 + \ln \left(\frac{\vartheta_i^c}{\sum_j x_j \vartheta_j^c} \right) - \frac{\vartheta_i^c}{\sum_j x_j \vartheta_j^c} \quad (11)$$

being ϑ_j^c the number of atoms (non hydrogen atoms) in the molecule j . The residual part is determined as follow,

$$\ln \gamma_i^{\text{Resid}} = \sum_k \vartheta_{ki} \left(\ln \Gamma_k - \ln \Gamma_k^i \right) \quad (12)$$

being ϑ_{ki} the number of atoms (non hydrogen atoms) in group k in molecule i , Γ_k the group activity coefficient of group k and Γ_k^i the activity coefficient of group k in a standard state (pure component i). The ASOG model considers the group activity coefficient is given by the Wilson equation as follows,

$$\ln \Gamma_k = 1 - \ln \left(\sum_l X_l a_{lk} \right) - \sum_m \frac{X_l a_{lm}}{\sum_m X_m a_{lm}} \quad (13)$$

where X_l represent the group fraction of group l in the liquid solution. In the above expression (Eq. 13) the summations extend over all groups and a_{lk} , a_{lm} are the group interaction parameters.

The UNIFAC^{8,10-12} models are generally based on the equations of the UNIQUAC model for the combinatorial part, being for the classical UNIFAC⁸ model,

$$\ln \gamma_i^{\text{Comb}} = \ln \left(\frac{\Phi_i}{x_i} \right) + q_i \left(\frac{Z}{2} \right) \ln \left(\frac{\theta_i}{\Phi_i} \right) + l_i - \left(\frac{\Phi_i}{x_i} \right) \sum_j x_j l_j \quad (14)$$

θ represents the molecular surface area fraction (see Eq. 9), Φ is the molecular volume fraction (see Eq. 9) and the pure-component lattice parameter, l , is function of van der Waals surface area (q) and van der Waals volume (r). For the mod. UNIFAC-Larsen¹⁰ model,

$$\ln \gamma_i^{\text{Comb}} = \ln \left(\frac{\Psi_i}{x_i} \right) + 1 - \frac{\Psi_i}{x_i} \quad (15)$$

Table 4 Results of predictions using group contribution models and PR-EOS

	mod. UNIFAC-Lyngby ¹⁰ OH/CCOO	UNIFAC-1991 ^{8,11} OH/CCOO	mod. UNIFAC-Dortmund ¹² OH/CCOO	ASOG-1979 ⁹ OH/CCOO	PR ¹³	PRSV ^{13,15}	PRWS ^{13,14}	PRSVWS ¹³⁻¹⁵
	methyl acetate (1) + 1-butanol (2) at 0.6 MPa							
MAD(y_i)	0.011	0.028	0.023	0.046	0.007	0.014	0.012	0.013
MAD(T)/K	0.93	3.32	2.76	5.93	0.82	0.47	0.37	0.45
MAD(p)/MPa	0.011	0.044	0.036	0.078				
MPD(y_i)	4.12	17.81	12.78	32.96				
MPD(y_2)	12.75	4.13	3.70	4.31				
	ethyl acetate (1) + 1-butanol (2) at 0.6 MPa							
MAD(y_i)	0.012	0.020	0.012	0.023	0.008	0.008	0.012	0.006
MAD(T)/K	1.17	2.16	0.70	2.39	0.74	0.38	0.55	0.26
MAD(p)/MPa	0.011	0.028	0.009	0.031				
MPD(y_i)	5.33	17.45	6.16	21.18				
MPD(y_2)	10.74	4.13	3.51	4.2				

$$\text{MPD}(F) = \frac{100}{n-2} \sum_{i=1}^n \frac{|F_{\text{exp}} - F_{\text{cal}}|}{F_{\text{exp}}}$$

where ψ represent the modified group volume fraction. For the mod. UNIFAC-Gmehling¹² model,

$$\ln \gamma_i^{\text{Comb}} = \ln \delta_i + 1 - \delta_i - q_i \left(\frac{Z}{2} \right) \left[\ln \left(\frac{\Phi_i}{\eta_i} \right) + 1 - \frac{\Phi_i}{\eta_i} \right] \quad (16)$$

being η the modified molecular surface area fraction and δ the modified molecular volume fraction. In the UNIFAC models, the residual part of the activity coefficient (Eq. 12 being ϑ_{ki} the number of groups of type k in molecule i ,) is replaced by the solution-of-groups concept. The following equation is used for the group activity coefficient,

$$\ln \Gamma_k = Q_k \left[1 - \ln \left(\sum_m \Theta_m \xi_{mk} \right) - \sum_m \frac{\Theta_m \xi_{mk}}{\sum_n \Theta_n \xi_{mn}} \right] \quad (17)$$

where Q_k is the van der Waals surface area of group k , Θ represents the group surface area fraction and ξ is defined by an equation that includes the group contribution parameters. Both Θ and ξ have different expressions in the UNIFAC versions.

Table 4 shows prediction results from the group contribution models. Figs. 4 and 5 show the experimental data and the fitting curves of predictions when using these group contribution models.

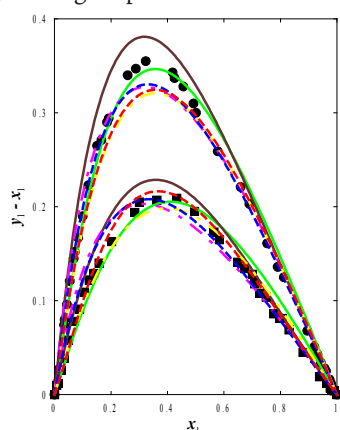


Fig. 4 Plot of experimental VLE data for MA1B (●) and EA1B (■) at 0.6 MPa together with predictions of mod. UNIFAC-Larsen¹⁰ (—, green color line); mod. UNIFAC-Gmehling¹² (—, dark brown color line); PR-EOS¹³ (—, blue color line); PRSVWS-EOS¹³⁻¹⁵ (—, red color line); PRWS-EOS^{13,14} (—, magenta color line) and PRSV-EOS^{13,15} (—, yellow color line).

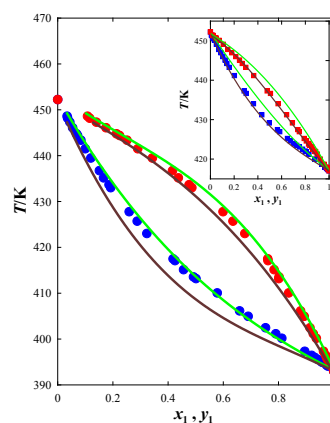


Fig. 5 Representation of experimental T - x_1 - y_1 data for the binary systems MA1B (●, ●) and EA1B (■, ■) at 0.6 MPa together with (green color lines) mod. UNIFAC-Larsen¹⁰ and (dark brown color lines) mod. UNIFAC-Gmehling¹² predictions.

In general terms, the best prediction for γ_i was obtained with the mod. UNIFAC model proposed by Gmehling et al.¹² However, most accurate results in composition were found using the mod. UNIFAC model proposed by Larsen et al.¹⁰ The Gmehling et al.¹² version also returns a good prediction for EA1B. The UNIFAC model⁸ with the Hansen et al.¹¹ parameters and the ASOG model⁹ yield poor predictions and higher deviations in pressure and temperature, being the mean proportional deviation (MPD) for the prediction of the vapor phase mole fraction, respectively: 9% and 16% for MA1B and 12% and 14% for EA1B.

Results indicate that with the current parameters, some of the group contribution models do not reproduce adequately the VLE at moderate pressures; however, it is often observed that predictions given by the models proposed by Larsen et al.¹⁰ and Gmehling et al.¹² are more successful.

Modelling with PR-EOS

The reliability in VLE modelling for mixtures that have hydrogen bonding via proton donor and proton acceptor is low if proper binary interaction parameters are not employed, especially at high pressure. Consequently, the prediction of phase equilibrium can be done by using EOS; if necessary, using the appropriate mixing rules. This is why in this work the

PR-EOS¹³ using quadratic mixing rules and the WS¹⁴ mixing rules have been used. The adjustable parameter employed by SV¹⁵ in the attractive term was also applied. The PR-EOS¹³ has the following equation:

$$p = \frac{RT}{v-b} - \frac{a(T)}{v(v+b)+b(v-b)} \quad (18)$$

where p , T and R represent pressure, temperature and the ideal gas constant. Furthermore, a is the temperature-dependant attractive parameter and b is the temperature-independent repulsive parameter, which are determined by the following equations:

$$p = \frac{RT}{v-b} - \frac{a(T)}{v(v+b)+b(v-b)} \quad (19)$$

$$p = \frac{RT}{v-b} - \frac{a(T)}{v(v+b)+b(v-b)} \quad (20)$$

being T_c and P_c respectively, the critical temperature and pressure of each pure component. The classical correlation for temperature-dependant β function is:

$$\beta(T) = \left[1 + m(1 - T_r^{0.5})\right]^2 \quad (21)$$

$$m = 0.37464 + 1.54226\omega - 0.26992\omega^2 \quad (22)$$

When the SV¹⁵ equation is employed, in PRSV-EOS m is modified according to Eq. 23, where κ_0 is a function of the acentric factor, and ω and κ_1 are adjustable parameters for each pure component, as follows:

$$m = \kappa_0 + \kappa_1(1 + T_r^{0.5})(0.7 - T_r) \quad (23)$$

$$\kappa_0 = (0.378893 + 1.4897153\omega - 0.17131848\omega^2 + 0.0196554\omega^3) \quad (24)$$

The classical mixing rules, with the binary interaction parameter $k_{1,ij}$ and $k_{2,ij}$ were employed. Therefore, the a_m and b_m parameters were:

$$a_m = \sum_i \sum_j x_i x_j (a_i a_j)^{0.5} (1 - k_{1,ij}) \quad (25)$$

$$b_m = \sum_i \sum_j x_i x_j \left(\frac{b_i + b_j}{2}\right) (1 - k_{2,ij}) \quad (26)$$

However, for non-ideal mixtures like those this paper the quadratic mixing rules can not to be adequate. Therefore, the WS¹⁴ mixing rules were also applied. The WS mixing rules are given by:

$$b_m = \frac{\sum_i \sum_j x_i x_j (b_{ij} - a_{ij} / (RT))}{\left(1 - \frac{A_\infty^E}{C} / (CRT) - \sum_i x_i a_i / (RT b_i)\right)} \quad (27)$$

$$(b_{ij} - a_{ij} / (RT)) = \frac{1}{2} [(b_i - a_i / (RT)) + (b_j - a_j / (RT))] (1 - k_{ij}) \quad (28)$$

$$a_m = b_m \left(\sum_i x_i \frac{a_i}{b_i} + \frac{A_\infty^E}{C} \right) \quad (29)$$

where C is a numerical constant equal to 1 and $k_{ij} = k_{ji}$ is the binary interaction parameter for each system. A_∞^E is an excess Helmholtz free energy model at infinite pressure that can be equated to a low-pressure excess Gibbs energy model²⁶. In this study, the NRTL model²³ was used, as follows:

$$\frac{A_\infty^E}{RT} = \sum_i x_i \frac{\sum_j x_j G_{ji} \tau_{ji}}{\sum_r x_r G_{ri}} \quad \text{with} \quad G_{ij} = \exp(-\alpha_{ij} \tau_{ij}) \quad (30)$$

being $\alpha_{ij} = \alpha_{ji}$ as well as τ_{ij} and τ_{ji} adjustable parameters to obtain agreement between theory and experiment for VLE. The non-randomness parameter (α) of the NRTL model²³ was fixed to 0.47 in this study.

Vapor pressures reported in literature^{1,20,21} were used to obtain the k_1 adjustable parameter of SV¹⁵ using the PR equation. The critical properties employed (see Table 2) were taken from Daubert and Danner¹⁹. SD was used for minimization parameters.

The Matlab program from Martin et al.²⁷ is an educational program with a library of different EOS's including PR¹³, PRSV^{13,15}, PRWS^{13,14} and PRSVWS¹³⁻¹⁵. We developed a FORTRAN code, based on a simplified version of the above-mentioned Matlab program, but related by separate to PR-EOS¹³, PRSV-EOS^{13,15}, PRWS-EOS^{13,14} and PRSVWS-EOS¹³⁻¹⁵.

Martin's Matlab program²⁷ uses inner functions, such as $fzero$, $fsolve$ or $fminsearch$. These inner math functions of Matlab are robust and reliable but they imply long times of computer use. We substitute them for our own FORTRAN subroutines that lead us to similar accuracy. At the same time, we change Matlab programs structure, avoiding unnecessary loops, and eliminating redundant assignment sentences, improving our FORTRAN code in speed of execution.

Using these new programs, our results are $k_1=0.0234$ ($k_1=0.05791^{28}$) with $SD=3.27$ and $MPD=1.6$ for methyl acetate; $k_1=0.0692$ ($k_1=0.06464^{28}$) with $SD=5.40$ and $MPD=1.2$ for ethyl acetate and $k_1=0.4874$ ($k_1=0.33431^{15}$) with $SD=4.43$ and $MPD=1.7$ for 1-butanol.

When comparing the results with those cited in the literature^{15,28}, a good match for the ethyl acetate and discrepancies in the other two substances is observed. However, while in the case of 1-butanol the temperature range used in this study for correlations is wider, in all cases the number of data used in this paper to obtain the SV parameter, is also much higher; this, along with the considerable differences in both the critical properties and acentric factor used in the case of methyl acetate and 1-butanol, can explain the differences.

The binary interaction parameters for the systems of this work were treated as fitting parameters of VLE data. The physical properties from literature¹⁹ were used for data processing by PR-EOS¹³ considering the classical $b(T)$ function for the attractive interaction and also by PRSV-EOS^{13,15} using the SV modification. In both cases, the numerical values of $k_{1,ij}$, $k_{2,ij}$ with quadratic mixing rules were obtained. In addition, the numerical values of $k_{1,ij}$, $k_{2,ij}$ were also calculated when the WS¹⁴ mixing rules and κ_{ij} , τ_{ij} , τ_{ji} parameters were employed in PRWS-EOS^{13,14} and PRSVWS-EOS¹³⁻¹⁵. All calculated values were obtained by using the FORTRAN programs above mentioned.

To systematize data analysis of the MA1B and EA1B binary systems, it was decided to obtain the acentric factor, since the models are highly dependent on this parameter. Vapor pressures from literature^{1,20,21} and the critical properties of Daubert and Danner¹⁹ were used. The Nelder and Mead method²⁵ was employed for data correlation. Results were: $\omega=0.328$ ($\omega=0.3253^{19}$) with $SD=0.0004$; $\omega=0.362$ ($\omega=0.3611^{19}$) with $SD=0.0012$ and $\omega=0.599$ ($\omega=0.5945^{19}$) with $SD=0.0003$, for methyl acetate, ethyl acetate and 1-butanol, respectively.

To predict the compositions of the MA1B and EA1B binary systems at 0.6 MPa it was considered the p-x₁ bubble point scheme. The simplex method²⁵ was used, and the objective function (OF) was as follows:

$$OF = \frac{1}{U(T)} \sum_1^n |T^{\text{exp}} - T^{\text{calc}}| + \frac{1}{U(y_1)} \sum_1^n |y_1^{\text{exp}} - y_1^{\text{calc}}| \quad (31)$$

Often for the Eq. 31 the maximum-likelihood principle is considered. Therefore, the standard deviations (SD) are employed. However, in this work uncertainties U(T); U(y₁) have been used in Eq. 31. This amendment arises when considering that SD is a standard uncertainty, and therefore, its use may be sufficient when the experimental data are correlated with the equations of the thermodynamic-mathematical models that enable the production of adjustable parameters. In addition, when the models can predict VLE data, it seems more reasonable to consider a higher level of confidence. That is why we have selected the expanded uncertainty, because in this way we ensure a higher quality prediction by the models.

Temperature and composition of vapor phase were compared with the theoretical predictions of VLE using the PR-EOS¹³, PRSV-EOS^{13,15}, PRWS-EOS^{13,14} and PRSVWS-EOS¹³⁻¹⁵. Table 4 presents the global results obtained for MAD(y₁) and MAD(T). On the other side, the results for binary interaction parameters and objective function obtained using PR-EOS¹³ were k₁=0.0345, k₂=-0.0354, OF=2.9 for MA1B system, and k₁=0.0319, k₂=0.0109, OF=2.8 for EA1B system; using PRSV-EOS^{13,15} the results were k₁=0.0231, k₂=0.0234, OF=2.0 for MA1B system, and k₁=0.0099, k₂=0.0901, OF=1.6 for EA1B system; using PRWS-EOS^{13,14} the results were k_{ij}=0.1519, α=0.47, τ_{ij}=-0.7693, τ_{ji}=1.4983, OF=1.6 for MA1B system, and k_{ij}=0.0588, α=0.47, τ_{ij}=-0.2311, τ_{ji}=0.8075, OF=2.3 for EA1B system. and using PRSVWS-EOS¹³⁻¹⁵ the results were k_{ij}=0.1269, α=0.47, τ_{ij}=0.0183, τ_{ji}=0.0258, OF=1.9 for MA1B system, and k_{ij}=0.4896, α=0.47, τ_{ij}=-0.4529, τ_{ji}=-0.7123, OF=1.1 for EA1B system. Figs. 4, 6, 7 show the experimental data and the correlation curves obtained by using these EOS.

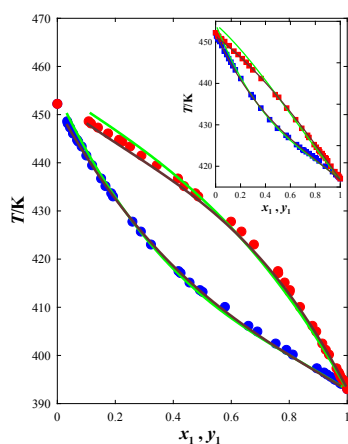


Fig. 6 Representation of experimental $T-x_1-y_1$ data for the binary systems MA1B (●, ●) and EA1B (■, ■) at 0.6 MPa. Predictions represented by green color lines and dark brown color lines using PR-EOS¹³ and PRSVWS-EOS¹³⁻¹⁵ respectively.

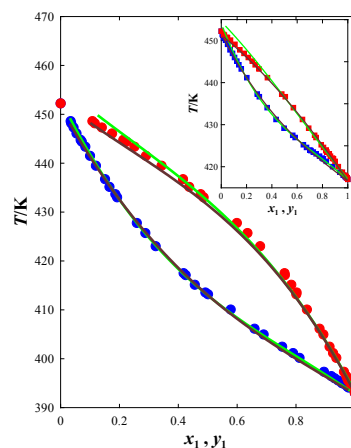


Fig. 7 Representation of experimental $T-x_1-y_1$ data for the binary systems MA1B (●, ●) and EA1B (■, ■) at 0.6 MPa. Predictions represented by green color lines and dark brown color lines using PRWS-EOS^{13,14} and PRSV-EOS^{13,15} respectively.

Results indicate that the best overall prediction of the experimental VLE data in both systems is obtained with the PRSVWS-EOS model¹³⁻¹⁵ as can be seen in Table 3 and Figs. 4 and 6. The PR-EOS model¹³ returns reasonably good predictions when considering the composition of the vapor phase (see Fig. 4). The prediction of temperature for both systems is poor (see Fig. 6), when compared to the results obtained with models that use the SV equation¹⁵. This can be observed in Figs. 4, 6, 7. On the other hand, in Fig. 4 a similar prediction of the composition of the vapor phase is observed with the PR-EOS¹³ and PRSVWS-EOS¹³⁻¹⁵ models. Fig. 6 shows that best temperature predictions are archived by using the SV equation¹⁵. A similar behavior can be seen in Figs. 4 and 7.

Therefore, in general, when the SV equation is employed, better predictions are obtained than when the PR model is used. However, this does not seem enough to describe the thermodynamic behavior, nor for VLE calculations. Nevertheless, when using the WS mixing rules, results show that the PRSVWS model can satisfactorily represent the VLE, for non-ideal polar organic systems, such as the ester + alcohol mixtures of this work.

CONCLUSIONS

Experimental data for the binary mixtures methyl acetate/1-butanol and ethyl acetate/1-butanol at 0.6 MPa were obtained. The thermodynamic consistency was verified by using the point-to-point test. Results satisfy the global criterion of this test. In addition, data obtained in this work shows good agreement with bibliographic data.

Predictions by using the ASOG and UNIFAC group contribution models were obtained. Results show that the mod. UNIFAC-Lingby version returns satisfactory and best predictions, although the mod. UNIFAC-Dortmund model returns a good prediction of EA1B.

Experimental data were correlated with PR-EOS using quadratic mixing rules and the Wong-Sandler mixing rules. The effect on the attractive term using

the Stryjek-Vera parameter was also verified. Globally, results show the best predictions were obtained by using the Stryjek-Vera parameter and Wong-Sandler mixing rules simultaneously.

AUTHOR INFORMATION

Funding

This work was supported by the authors. This work has not financial support of the Spanish government.

Notes

The authors declare no competing financial interest.

REFERENCES

1. Susial, P.; Sosa-Rosario, A.; Rodríguez-Henríquez, J.J.; Rios-Santana, R. Vapor Pressures and VLE Data Measurements. Ethyl Acetate+Ethanol at 0.1, 0.5 and 0.7 MPa Binary System. *J. Chem. Eng. Jpn.* **2011**, *44*, 155–163.
2. Susial, P.; García-Vera, D.; Susial, R.; Castillo, V.D.; Estupiñan, E.J.; Apolinario, J.C.; Rodríguez-Henríquez, J.J. Experimental Determination of Vapor–Liquid Equilibria. Binary Systems of Methyl Acetate, Ethyl Acetate and Propyl Acetate with 1-Propanol at 0.6 MPa. *J. Chem. Eng. Data* **2013**, *58*, 2861–2867.
3. Gmehling, J.; Onken, U. *Vapor-Liquid Equilibrium Data Collection*; Dechema: Frankfurt, 2008; Vol. 1, Part. 2j; pp 41–51 and 104–109.
4. Gmehling, J.; Onken, U.; Rarey-Nies, J.R. *Vapor-Liquid Equilibrium Data Collection*; Dechema: Frankfurt, 1990; Vol. 1, Part. 2f; pp 137 and 145–146.
5. Susial, P.; Estupiñan, E.J.; Castillo, V.D.; Rodríguez-Henríquez, J.J.; Apolinario, J.C. Experimental Determination of Densities and Isobaric Vapor–Liquid Equilibria of Methyl Acetate and Ethyl Acetate with Alcohols (C3 and C4) at 0.3 MPa. *Int. J. Thermophys* **2013**, *34*, 1906–1917.
6. Gmehling, J.; Onken, U.; Arlt, W. *Vapor-Liquid Equilibrium Data Collection*; Dechema: Frankfurt, 1990; Vol. 1, Part. 2b; p 148.
7. Van Ness, H.C.; Byer, S.M.; Gibbs, R.E. Vapor-Liquid Equilibrium: I. An Appraisal of Data Reduction Methods. *AIChE J.* **1973**, *19*, 238–244.
8. Fredenslund, A.; Gmehling, J.; Rasmussen, P. *Vapor-liquid Equilibria Using UNIFAC. A Group Contribution Model*; Elsevier: Amsterdam, 1977; pp 11–15, 73 and 214–219.
9. Kojima, K.; Tochigi, K. *Prediction of Vapor-Liquid Equilibria by the ASOG Method*; Kodansha Ltd.: Tokyo, 1979; pp 11–50.
10. Larsen, B.L.; Rasmussen, P.; Fredenslund, A. A Modified UNIFAC Group-Contribution Model for Prediction of Phase Equilibria and Heats of Mixing. *Ind. Eng. Chem. Res.* **1987**, *26*, 2274–2286.
11. Hansen, H.K.; Rasmussen, P.; Fredenslund, A.; Schiller, M.; Gmehling, J. Vapor-Liquid Equilibria by UNIFAC Group-Contribution. 5. Revision and Extension. *Ind. Eng. Chem. Res.* **1991**, *30*, 2352–2355.
12. Gmehling, J.; Li J.; Schiller, M. A Modified UNI
13. FAC Model. 2. Present Parameter Matrix and Results for Different Thermodynamic Properties. *Ind. Eng. Chem. Res.* **1993**, *32*, 178–193.
14. Peng, D.Y., Robinson, D.B. A new two-constant equation of state. *Ind. Eng. Chem. Fundam.* **1976**, *15*, 59–64.
15. Wong, D.S.H, Sandler, S.I. A Theoretically Correct Mixing Rule for Cubic Equations of State. *AIChE J.* **1992**, *38*, 671–680.
16. Stryjek, R.; Vera, J.H. PRSV: An improved Peng–Robinson equation of state for pure compounds and mixtures. *Can. J. Chem. Eng.* **1986**, *64*, 323–333.
17. Susial, P.; Rios-Santana, R.; Sosa-Rosario, A. VLE Data of Methyl Acetate + Methanol at 1.0, 3.0 and 7.0 bar with a New Ebulliometer. *J. Chem. Eng. Jpn.* **2010**, *43*, 650–656.
18. Hayden, J.G.; O’Connell, J.P. A Generalised Method for Predicting Second Virial Coefficients. *Ind. Eng. Chem. Process Des. Dev.* **1975**, *14*, 209–216.
19. Yen, L.C.; Woods, S.S. A generalized equation for computer calculation of liquid densities. *AIChE J.* **1966**, *12*, 95–99.
20. Daubert, T.E.; Danner, R.P. *Physical and Thermodynamic Properties of Pure Chemicals: Data Compilation*; Hemisphere Publishing Co.: New York, 1989; Vol. 2.
21. Susial, P.; Susial, R.; Estupiñan, E.J.; Castillo, V.D.; Rodríguez-Henríquez, J.J.; Apolinario, J.C. Determination and thermodynamic evaluation of isobaric VLE of methyl acetate or ethyl acetate with 2-propanol at 0.3 and 0.6 MPa. *Fluid Phase Equilibria* **2014**, *375*, 1–10.
22. Susial, P.; Rodríguez-Henríquez, J.J.; Castillo, V.D.; Estupiñan, E.J.; Apolinario, J.C.; Susial, R. Isobaric (vapor + liquid) equilibrium for n-propyl acetate with 1-butanol or 2-butanol. Binary mixtures at 0.15 and 0.6 M. *Fluid Phase Equilib.* **2015**, *385*, 196–204.
23. Wilson, G.M. Vapor-Liquid Equilibrium. XI. A New Expression for the Excess Free Energy of Mixing. *J. Am. Chem. Soc.* **1964**, *86*, 127–130.
24. Renon, H., Prausnitz, J.M. Local compositions in thermodynamic excess functions for liquid mixtures. *AIChE J.* **1968**, *14*, 135–144.
25. Abrams, D.S.; Prausnitz, J.M. Statistical Thermodynamics of Liquid Mixtures: A New Expression for the Excess Gibbs Energy of Partly or Completely Miscible Systems. *AIChE J.* **1975**, *21*, 116–128.
26. Nelder, J.; Mead, R. A simplex method for function minimization. *Comput. J.* **1965**, *7*, 308–313.
27. Wong, D.S.; Orbey, H.; Sandler, S.I. Equation-of-state Mixing Rule for Non-ideal Mixtures Using Available Activity Coefficient Model Parameters and That Allows Extrapolation over Large Ranges of Temperature and Pressure. *Ind. Eng. Chem. Res.* **1992**, *31*, 2033–2039.
28. Martín, A., Bermejo, M.D., Mato, F.A., Cocero, M.J. Teaching advanced equations of state in applied thermodynamics courses using open source programs. *Educ. Chem. Eng.* **2011**, *6*, e114–e121.
29. Proust, P.; Vera, J.H. PRSV: The Stryjek-Vera modification of the Peng-Robinson equation of state. Parameters for other pure compounds of industrial interest. *Can. J. Chem. Eng.* **1989**, *67*, 170–173.